JOURNAL OF Applied Polymer SCIENCE

Structure–Property Relationships of Hyperbranched Polyimide–Silica Hybrid Membranes with Different Degrees of Modification

Masako Miki, Tomoyuki Suzuki, Yasuharu Yamada
R&D Center for Nanomaterials and Devices, Kyoto Institute of Technology, Matsugasaki, Sakyo-Ku, Kyoto 606-8585, Japan
Correspondence to: Y. Yamada (E-mail: y-yamada@kit.ac.jp)

ABSTRACT: The physical and gas transport properties of hyperbranched polyimide (HBPI)–silica hybrid membranes with different degrees of modification prepared with a dianhydride, 4,4′-(hexafluoroisopropylidene) diphthalic anhydride, a triamine, 1,3,5-tris(4-aminophenoxy) benzene, and a coupling agent, 3-aminopropyltrimethoxysilane, were investigated. With increasing degree of modification, the inherent viscosity of the hyperbranched poly(amic acid) increased, and the density of the HBPI decreased; this suggested the formation of crosslinking through the coupling agent. Dynamic mechanical analysis and thermomechanical analysis measurements indicated that the mobility of the HBPI molecular chains decreased in the rubbery region and that the free-volume holes of the HBPI increased in the glassy region because of the increased degree of crosslinking through the coupling agent. The CO_2 permeability and CO_2/CH_4 permselectivity of the HBPI–silica hybrid membranes increased with increasing silica content, with the latter increase being remarkable for the HBPI–silica hybrid membranes with a higher degree of modification. This suggested that the pronounced improvement in the CO_2/CH_4 permselectivity of the highly modified HBPI–silica hybrid membranes was likely caused by the contributions of both the intrinsic high-fractional free volume attributed to crosslinking through the coupling agent and the characteristic distribution and interconnectivity of free-volume holes created by hybridization with silica. © 2013 Wiley Periodicals, Inc. J. Appl. Polym. Sci. 000: 000–000, 2013

KEYWORDS: composites; dendrimers; hyperbranched polymers and macrocycles; membranes; polyimides; structure–property relations

Received 29 October 2012; accepted 10 January 2013; published online
DOI: 10.1002/app.39011

INTRODUCTION

In recent years, a large number of studies on polymeric membranes for CO_2 separation have been performed because membrane separation is a key technology for combating global warming through the utilization of renewable energy and carbon dioxide capture and storage (CCS).[1] Aromatic polyimides have been of particular interest in gas separation membranes because of their excellent mechanical and thermal properties and high gas permeability and selectivity.[2–5]

Dendritic polymers (e.g., dendrimers or hyperbranched polymers) are high-performance polymers possessing unique properties compared with their linear analogues. They have good solubility, reduced viscosity, higher fractional free volume (FFV), and multifunctionality, which arises from multiple end groups. The most remarkable characteristic of dendritic polymers is that they have a large number of molecular terminal groups that can be modified to create different types of multifunctional polymers.[6,7] The synthetic methods used to prepare hyperbranched polymers can be divided into two major categories: (1) the self-polycondensation of A_x- or AB_x-type monomers and (2) the copolymerization of $A_x + B_y$ monomers. Hyperbranched polyimides (HBPIs) can be prepared from either the self-polycondensation of AB_2-type monomers or the polycondensation reaction of $A_2 + B_3$ monomers, where A_2 represents a dianhydride monomer and B_3 represents a triamine monomer. In the case of an $A_2 + B_3$ type polycondensation reaction, a variety of HBPIs can be synthesized by changing the monomer ratio and the combination of A_2 and B_3 monomers.[8,9] From this point of view, in recent years, many studies on the gas transport properties of HBPI membranes have been done.[10–12] Fang et al.[9,10] were the first to report the synthesis of HBPIs derived from a triamine, tris(4-aminophenyl)amine, and commercially available dianhydrides. They revealed that HBPI membranes showed good gas separation performance compared with linear-type polyimides. We[13] also studied the gas transport properties of HBPI membranes prepared by the polycondensation reaction of a triamine, 1,3,5-tris(4-aminophenoxy)benzene (TAPOB), and a dianhydride, 4,4′-(hexafluoroisopropylidene) diphthalic anhydride (6FDA), and found that the 6FDA–TAPOB HBPI membrane exhibited a high gas permeability and O_2/N_2 selectivity, which arose from its characteristic hyperbranched structure.

Organic–inorganic hybrid materials have been studied extensively because the newly combined materials offer the advantages of both an inorganic material (e.g., rigidity, thermal stability) and an organic polymer (e.g., flexibility, dielectric, ductility, processability).[14,15] The synthesis of polyimide–silica hybrid materials and the investigation of their physical and gas transport properties have also received much attention.[16–19] In previous research,[20–23] we studied the syntheses and gas transport properties of HBPI–silica hybrid membranes prepared with commercially available dianhydride monomers and several kinds of triamine monomers and found that these membranes showed characteristics quite different from conventional polymer membranes. Specifically, the gas permeability and CO_2/CH_4 selectivity of HBPI–silica hybrid membranes prepared by a sol–gel reaction with tetramethoxysilane (TMOS) increased with increasing silica content without any dependence on the molecular structure; this suggested the characteristic distribution and interconnectivity of free-volume holes created by the incorporation of silica.[20–23] In hybridization, we also modified a part of the molecular terminals of the HBPIs with a silane coupling agent to enhance the compatibility between the HBPI and silica and, thereby, to improve the dispersability of the silica element. Some of the alkoxysilyl groups introduced into the molecular terminals may have crosslinked with each other. At this stage, there are no data pertinent to the physical and gas transport properties of HBPI–silica hybrid membranes with different degrees of modification.

The objective of this study was to prepare and characterize HBPI–silica hybrid membranes with different degrees of modification; we expected that an increased degree of modification would lead to improved characteristics and gas transport properties in the HBPI–silica hybrids.

EXPERIMENTAL

Materials

TAPOB was synthesized by the reduction of 1,3,5-tris(4-nitrophenoxy)benzene with palladium carbon and hydrazine in methanol.[24] 6FDA was kindly supplied by Daikin Industries (Osaka, Japan). TMOS was purchased from AZmax, Co., Ltd. (Ichihara City, Japan), and 3-aminopropyltrimethoxysilane (APTrMOS) was purchased from Sigma Aldrich (St. Louis, MO). *N,N*-Dimethylacetamide (DMAc) used as a solvent was purchased from Nacalai Tesque (Kyoto, Japan). The chemical structures of the monomers and alkoxysilanes are shown in Figure 1.

Polymerization

An amount of 3 mmol of 6FDA was dissolved in 40 mL of DMAc in a 100-mL three-necked flask under N_2 flow at room temperature. An amount of 1.6 mmol of TAPOB in 20 mL of DMAc was then added dropwise through a syringe with stirring. After 3 h of stirring, the reaction mixture was diluted to a 2 wt % solid concentration to prevent gelation. Subsequently, an arbitrary quantity of the silane coupling agent, APTrMOS, was added to the reaction mixture to modify the end groups of the hyperbranched poly(amic acid)s (HBPAAs) with different ratios. After 1 h of stirring, 6FDA–TAPOB HBPAA was obtained.

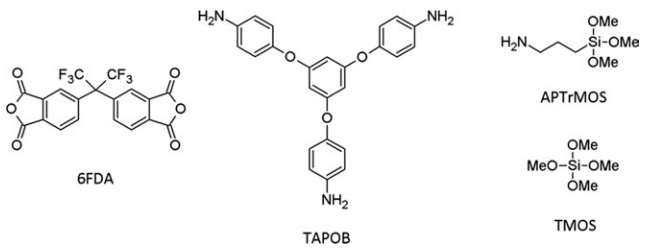

Figure 1. Chemical structures of the monomers, silane coupling agent, and alkoxysilane.

Membrane Formation

The 6FDA–TAPOB HBPI–silica hybrid membranes were prepared by the reaction of HBPAAs with alkoxysilane and TMOS by a sol–gel reaction; this was followed by thermal imidization. Appropriate amounts of TMOS and a drop of 1*N*-HCl were added to the DMAc solution of the HBPAAs. The mixed solutions were stirred for 24 h, then cast on PET films, and dried at 85°C for 3 h. The prepared membranes were peeled off and subsequently imidized and hybridized at 100°C for 1 h, 200°C for 1 h, and 300°C for 1 h in a heating oven under an N_2 flow. The average thickness of the HBPI–silica hybrid membranes was about 30 μm.

Measurements

The inherent viscosity (η_{inh}) was measured in a DMAc solution with a 0.5 g/dL concentration at 25°C with an Ubbelohde viscometer. Attenuated total reflection (ATR)–Fourier transform infrared (FTIR) spectra were recorded on a Jasco (Easton, MD) FT/IR-4100 instrument in the wave-number range 550–4000 cm^{-1} at a resolution of 1 cm^{-1}. Ultraviolet–visible optical transmittances were measured with a Jasco V-530 ultraviolet–visible spectrometer at wavelengths of 200–800 nm. Thermogravimetric (TG)–differential thermal analysis (DTA) experiments were performed with a Seiko Instruments (Chiba, Japan) TG/DTA5200 instrument at a heating rate of 10°C/min under an air flow. Dynamic mechanical analysis (DMA) measurements were performed with a Seiko Instruments DMA6100 instrument at a heating rate of 5°C/min under an N_2 flow; the load frequency was 1 Hz. Thermomechanical analysis (TMA) measurements were carried out with a Seiko TMA/SS6100 at a heating rate of 5°C/min under an N_2 flow. The density (ρ) of the pure HBPIs was measured by a floating method with bromoform and 2-propanol at 25°C. According to the group contribution method, the FFV of a polymer can be estimated by the following equation:[25]

$$\mathrm{FFV} = \frac{V_{sp} - 1.3V_w}{V_{sp}} \tag{1}$$

where V_{sp} (cm^3/mol) is the specific molar volume and V_w (cm^3/mol) is the van der Waals volume of the repeat unit.

CO_2, O_2, N_2, and CH_4 permeation measurements were taken with a constant volume/variable pressure apparatus under 76 cmHg at 25°C. The permeability coefficient {P [cm^3(STP)cm/cm^2 s cmHg]} was determined by the following equation:[26]

$$P = \frac{22414}{A}\frac{L}{p}\frac{V}{RT}\frac{dp}{dt} \tag{2}$$

where A is the membrane area (cm^2), L is the membrane thickness (cm), p is the upstream pressure (cmHg), V is the

downstream volume (cm^3), R is the universal gas constant (6236.56 cm^3 cmHg/mol K), T is the absolute temperature (K), and dp/dt is the permeation rate (cmHg/s). The gas P could be explained on the basis of the solution–diffusion mechanism, which is represented by the following equation:[27,28]

$$P = DS \tag{3}$$

where D (cm^2/s) is the diffusion coefficient and S [cm^3(STP)/cm^3_{polym} cmHg] is the solubility coefficient. The diffusion coefficient was calculated by the time-lag method represented by the following equation:[29]

$$D = \frac{L^2}{6\theta} \tag{4}$$

where θ (s) is the time lag.

RESULTS AND DISCUSSION

Polymer Synthesis

Two types of HBPIs can be prepared by a different addition orders and molar ratios of each monomer in the synthesis of HBPI by an $A_2 + B_3$ type polycondensation reaction.[9] In this study, the triamine solution was added to the dianhydride solution with a triamine and dianhydride monomer molar ratio of 1:2; we thus obtained dianhydride-terminated HBPIs. Subsequently, an arbitrary quantity of the silane coupling agent APTrMOS was added to the reaction mixture to prepare three kinds of HBPAAs with different terminal modification rates. In the 6FDA–TAPOB system, a three-dimensional intermolecular crosslinking reaction occurred easily because of the high reactivity of the 6FDA monomers and the equivalent reactivity of the three amino groups of TAPOB. However, a series of HBPAAs were successfully prepared without gelation by the control of the reaction conditions, mainly the monomer concentrations in this study. HBPI–silica hybrid membranes were prepared by a sol–gel reaction with HBPAA, TMOS, water, and hydrochloric acid as a catalyst, followed by thermal imidization. A schematic representation of the HBPI–silica hybrid is shown in Figure 2. The η_{inh} values of HBPAA are shown in Table I and are plotted against the degrees of modification in Figure 3. η_{inh} increased with increasing degree of modification; this suggested an increase in the molecular weight by crosslinking through the coupling agent.

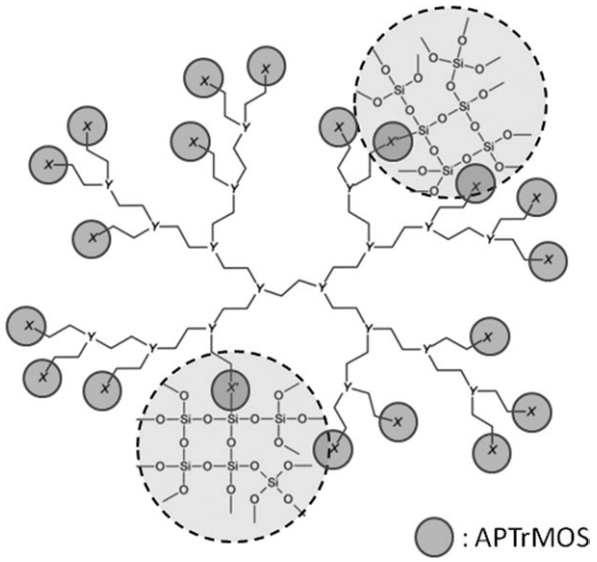

Figure 2. Schematic representation of the HBPI–silica hybrid.

Polymer Characterization

The HBPI ρs, listed in Table I, decreased with increasing degree of modification. This indicated that the HBPI molecular chains were difficult to pack by crosslinking through the coupling agent.

Table I. Physical Properties of the HBPI–Silica Hybrid Films

				TG-DTA		DMA	TMA	
	η_{inh} (dL/g)	ρ (g/cm^3)	Transmittance at 600 nm (%)	T_d^5 (°C)	Residue (%)	T_g (°C)	CTE ($<T_g$; ppm/°C)	CTE ($>T_g$; ppm/°C)
6FDA-TAPOB-APTrMOS (0/3)	0.33	1.439	88.3	484.4	0	278.6	51	4345
6FDA-TAPOB-APTrMOS (1/3)	0.34	1.429	89.7	468.6	0	292.8	52	1679
10 wt % SiO_2	—	—	92.9	487.7	10	315.5	49	730
20 wt % SiO_2	—	—	92.0	499.3	20	329.9	39	292
30 wt % SiO_2	—	—	93.0	507.5	32	340.7	31	123
6FDA-TAPOB-APTrMOS (2/3)	0.36	1.420	92.0	462.3	0	311.5	55	1352
10 wt % SiO_2	—	—	92.8	494.6	11	345.7	48	503
20 wt % SiO_2	—	—	91.2	502.3	22	356.4	36	148
30 wt % SiO_2	—	—	94.4	510.2	32	370.7	31	71
6FDA-TAPOB-APTrMOS (3/3)	0.40	1.411	91.8	459.6	1	330.9	58	984
10 wt % SiO_2	—	—	91.6	482.3	9	360.7	52	334
20 wt % SiO_2	—	—	91.9	500.0	21	376.1	45	132
30 wt % SiO_2	—	—	93.5	509.3	30	390.2	36	67

Applied Polymer SCIENCE

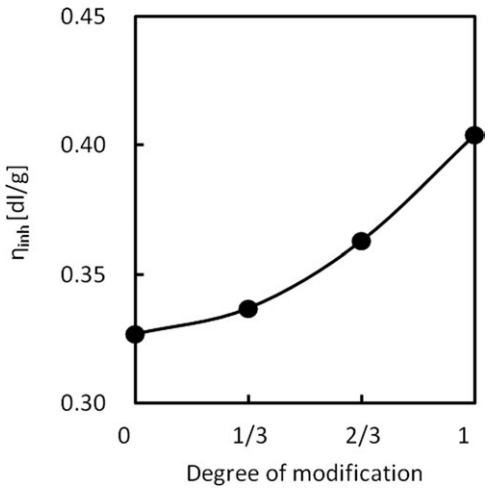

Figure 3. Relationship between the degree of modification and η_{inh} of HBPAA solutions.

The ATR–FTIR spectra of the HBPI membranes with different degrees of modification and the HBPI–silica hybrid membranes (degree of modification = 3/3) are shown in Figure 4(a,b). The bands observed around 1784 cm^{-1} (C═O asymmetrical stretching), 1720 cm^{-1} (C═O symmetrical stretching), 1374 cm^{-1} (C—N stretching), and 720 cm^{-1} (C═O bending) were characteristic absorption bands of polyimides.[10,30] In contrast, no characteristic bands of poly(amic acid)s around 1680 cm^{-1} were found. These results indicate that the prepared membranes were well imidized. The band around 1857 cm^{-1}, attributed to the terminal anhydride groups, decreased with increasing degree of modification; this indicated that the coupling agents reacted with the terminal anhydride groups quantitatively. For the HBPI–silica hybrid membranes, the bands observed around 1100 cm^{-1}, assigned to Si—O—Si stretching, increased with increasing silica content; this indicated sufficient formation of the three-dimensional Si—O—Si network [Figure 4(b)].[31] The broad absorption bands around 3480 cm^{-1} were likely due to the silanol groups remaining in the silica domain.

The optical transmittances of the HBPI–silica hybrid membranes are shown in Table I. These membranes had good transparency, which indicated a favorable dispersion of the silica nanoparticles. This high homogeneity resulted not only from the covalent bonds between HBPI and the silica domain formed by APTrMOS but also from the characteristic hyperbranched structure of the molecular chains.[32]

The thermal properties of the HBPI–silica hybrid membranes were investigated by TG–DTA, DMA, and TMA measurements. The 5% weight loss temperatures (T_d^5s) of the HBPI–silica hybrid membranes were investigated by TG–DTA and are summarized in Table I, along with the silica contents determined from the residues at 800°C. The residues showed that all of the hybrid membranes contained appropriate amounts of silica, as expected. In Figure 5, the T_d^5 values of the HBPI–silica hybrid membranes are plotted against the silica content. The T_d^5s of the HBPI membranes without silica decreased with increasing degree of modification. This was probably because the C—N bonds formed by the addition of APTrMOS were less thermally stable. The T_d^5s of the HBPI–silica hybrid membranes increased with increasing silica content. This increased the thermal stability of the HBPI–silica hybrid membranes resulting from the formation of crosslinking between HBPI and the silica domain, the introduction of inorganic characteristics, and the radical trap effect of silica.

The storage moduli (E's) of the HBPI membranes with different degrees of modification are shown in Figure 6(a). In the rubbery region, the E' values of the HBPI membranes increased with increasing degree of modification. This result indicates that in the rubbery region, the mobility of the HBPI molecular chains decreased because of the increased degree of crosslinking

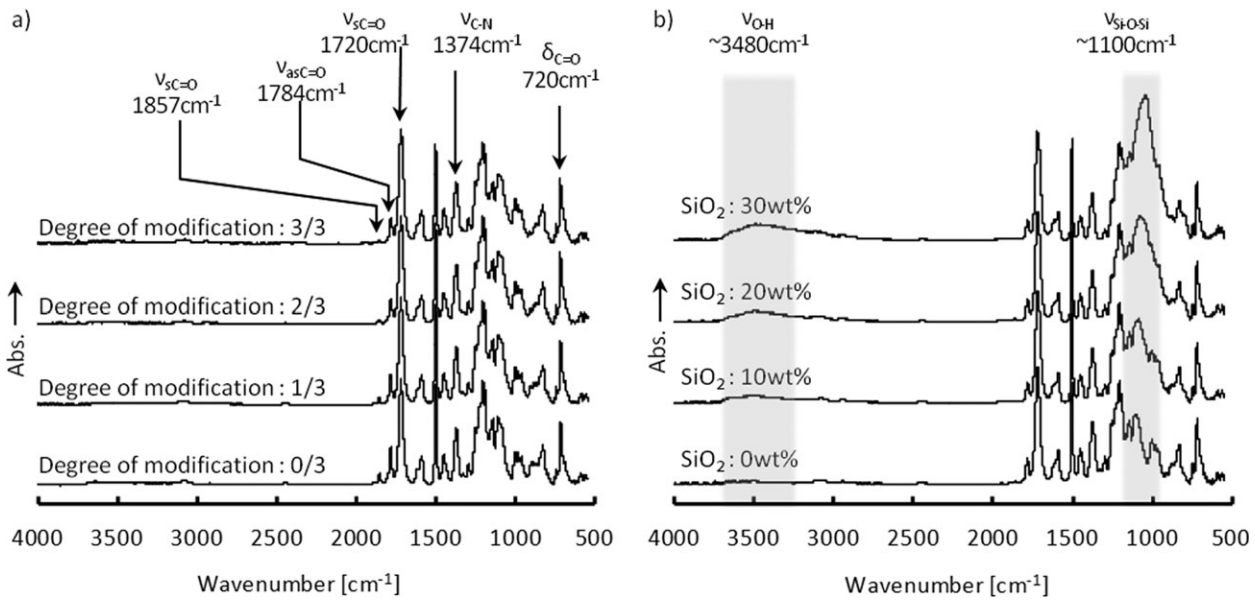

Figure 4. ATR–FTIR spectra of the (a) HBPI and (b) HBPI–silica hybrid membranes (degree of modification = 3/3).

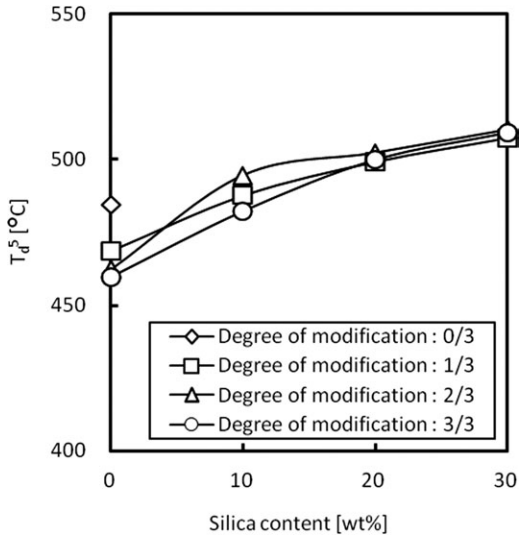

Figure 5. T_d^5 values of the HBPI–silica hybrids.

through the coupling agent. In contrast, in the glassy region, E' decreased with increasing degree of modification. This was because in the glassy region, the HBPI molecular chains were difficult to pack by crosslinking through the coupling agent; this led to an enlargement of the free-volume holes.[33] E' of the HBPI–silica hybrid membranes increased with increasing silica content in both regions [Figure 6(b)]. This increase was caused by the increase in the inorganic behavior and the decrease in the mobility of the HBPI molecular chains by hybridization with silica.

The glass-transition temperatures (T_g's) of the HBPI–silica hybrid membranes determined from the peak top of tan δ are summarized in Table I and are plotted against the silica content in Figure 7. When the degree of modification and the silica content were increased, the T_g's shifted to higher temperatures, along with a decrease in the peak intensity and a broadening of the half-width of tan δ. This result indicated that the T_g's increased with increasing inorganic behavior and decreasing mobility of the HBPI molecular chains caused by crosslinking through the coupling agent and/or silica domains.

The coefficients of thermal expansion (CTEs) of the HBPI membranes with different degrees of modification are listed in Table I and are plotted against the degree of modification in Figure 8. CTEs in the glassy region increased with increasing degree of modification. This result indicated that the free-volume holes of the HBPI increased in the glassy region because of the increase in the degree of crosslinking through the coupling agent. In contrast, the CTEs in the rubbery region decreased with increasing degree of modification. This result indicates that the mobility of the HBPI molecular chains decreases in the rubbery region because of the increase in the degree of crosslinking through the coupling agent.[33] For the HBPI–silica hybrid membranes, in both regions, the CTEs decreased with increasing silica content. This was also caused by the enhancement of the thermomechanical stability of the HBPI matrix through the formation of a robust three-dimensional Si—O—Si network and the decreased mobility of the HBPI molecular chains through hybridization with silica. The results obtained from DMA and TMA measurements were satisfactorily correlated.

Gas Transport Properties

The gas permeability, diffusion, and solubility coefficients of the HBPI–silica hybrid membranes with different degrees of modification are summarized in Table II, along with the FFV values calculated from the group contribution method. The gas P values and FFV values of the pure HBPI membranes without silica increased with increasing degree of terminal modification. This was due to the increased rigidity of the HBPIs by the formation of crosslinking through the coupling agent. The increase in FFV with increasing degree of modification supported the previous discussion about the decrease of E' and the increase in CTE in the glassy region.

Gas P values of the HBPI–silica hybrid membranes increased with increasing the silica content because of the contributions of the diffusion coefficient and the solubility coefficient. These results suggest the additional formation of free-volume holes and a

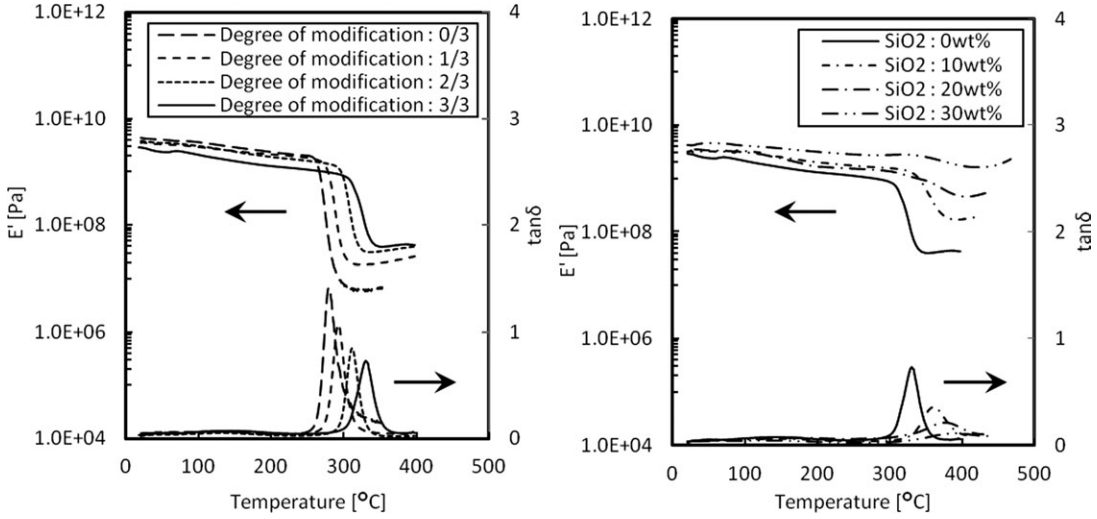

Figure 6. E' of the (a) HBPI and (b) HBPI–silica hybrid membranes (degree of modification = 3/3).

Applied Polymer SCIENCE

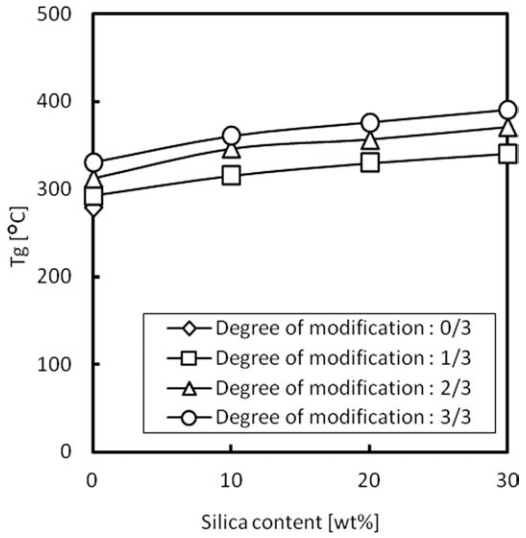

Figure 7. T_g's of the HBPI–silica hybrid membranes derived from the peak top of tan δ.

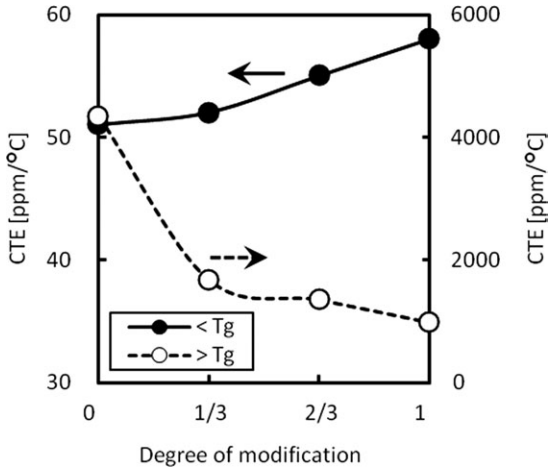

Figure 8. CTEs of the HBPI membranes.

Langmuir sorption site effective for gas transport properties through hybridization with silica.[13,34,35] Similar gas transport properties have been reported in several other studies. Park et al.[36] studied the gas permeation properties of siloxane containing polyimide–porous silica hybrid membranes and suggested that gas transport could occur through the porous silica network or in the interfacial region between the narrow silica networks and the organic matrix. With regard to the increase in the diffusion coefficient, Merkel et al.[37] studied a superglassy polymer-fumed silica nanocomposite and found that the relatively high free volume around the periphery of the silica particles, where the rigid polymer chains were unable to pack efficiently, caused the gas molecules to diffuse more rapidly compared to their movement in the bulk polymer. Boroglu and Gurkaynak[19] also reported that the P of the polyimide–siloxane hybrid polymer membranes increased with increasing siloxane content and suggested that the increased gas permeability resulted from the disturbed polymer chain packing and, thus, the increased free volume. The increased solubilities suggested that the Langmuir sorption site was additionally formed by the incorporation of silica domains. Takahashi et al.[38] reported that the poly(ether imide)–silica nanocomposite membranes showed an increase in the relative solubility when the SiO_2 content was increased; this was contrary to Maxwell's theory and suggested that these results may have reflected the presence of voids in addition to sorption in the matrix polymer and possibly some contribution of adsorption to the filler or at the filler–matrix interface. Garcia et al.[39] also reported that sorption in the carbon particles or at the interface of a particle–polymer increased the apparent solubility for poly(ether imide)–carbon composite membranes.

O_2/N_2 and CO_2/CH_4 Selectivities

The ideal permselectivity for the combination of gases A and B [α(A/B)] is defined by the equation:[40]

Table II. Gas Transport Properties of the HBPI–Silica Hybrid Membranes at 76 cmHg and 25°C

		$P \times 10^{10}$ [cm^3(STP)cm/cm^2 s cmHg]				$D \times 10^8$ (cm^2/s)				$S \times 10^2$ [cm^3(STP)/cm^3 of polymer cmHg]			
	FFV	CO_2	O_2	N_2	CH_4	CO_2	O_2	N_2	CH_4	CO_2	O_2	N_2	CH_4
6FDA-TAPOB-APTrMOS (0/3)	0.163	5.7	1.3	0.18	0.089	0.27	1.2	0.22	0.044	21	1.0	0.80	2.0
6FDA-TAPOB-APTrMOS (1/3)	0.164	7.9	1.6	0.24	0.11	0.35	1.4	0.28	0.030	22	1.1	0.86	3.5
10 wt %SiO_2	—	9.0	1.8	0.26	0.13	0.36	1.4	0.27	0.039	25	1.3	0.95	3.3
20 wt %SiO_2	—	11	2.0	0.30	0.13	0.36	1.4	0.25	0.028	30	1.5	1.2	4.8
30 wt %SiO_2	—	14	2.4	0.36	0.17	0.39	1.4	0.27	0.052	36	1.7	1.3	3.3
6FDA-TAPOB-APTrMOS (2/3)	0.164	11	2.1	0.32	0.17	0.43	1.6	0.33	0.051	25	1.3	0.99	3.4
10 wt % SiO_2	—	14	2.6	0.40	0.18	0.45	1.6	0.31	0.038	31	1.7	1.3	4.8
20 wt % SiO_2	—	14	2.5	0.38	0.20	0.42	1.5	0.27	0.042	34	1.7	1.4	4.9
30 wt % SiO_2	—	19	3.2	0.47	0.23	0.52	1.8	0.31	0.060	37	1.8	1.5	3.7
6FDA-TAPOB-APTrMOS (3/3)	0.165	14	2.7	0.42	0.24	0.51	1.9	0.34	0.058	27	1.4	1.2	4.0
10 wt % SiO_2	—	17	3.0	0.47	0.26	0.54	1.9	0.37	0.063	31	1.6	1.3	4.1
20 wt % SiO_2	—	19	3.2	0.52	0.23	0.53	1.9	0.36	0.047	36	1.7	1.4	5.0
30 wt % SiO_2	—	22	3.6	0.55	0.25	0.59	2.1	0.38	0.050	38	1.7	1.5	5.1

Table III. O_2/N_2 and CO_2/CH_4 Selectivities of the HBPI–Silica Hybrid Membranes at 76 cmHg and 25°C

	O_2/N_2 selectivity			CO_2/CH_4 selectivity		
	$\alpha(O_2/N_2)$	$\alpha^D(O_2/N_2)$	$\alpha^S(O_2/N_2)$	$\alpha(CO_2/CH_4)$	$\alpha^D(CO_2/CH_4)$	$\alpha^S(CO_2/CH_4)$
6FDA-TAPOB-APTrMOS (0/3)	7.1	5.6	1.3	64	6.2	10
6FDA-TAPOB-APTrMOS (1/3)	6.5	5.1	1.3	73	12	6.3
10 wt % SiO_2	6.8	5.2	1.4	68	9.2	7.6
20 wt % SiO_2	6.7	5.5	1.3	81	13	6.3
30 wt % SiO_2	6.8	5.3	1.3	83	7.5	11
6FDA-TAPOB-APTrMOS (2/3)	6.6	5.0	1.3	62	8.5	7.4
10 wt % SiO_2	6.5	5.1	1.3	76	12	6.5
20 wt % SiO_2	6.5	5.5	1.2	70	10	6.9
30 wt % SiO_2	6.8	5.8	1.2	85	8.6	10
6FDA-TAPOB-APTrMOS (3/3)	6.3	5.6	1.2	60	8.8	6.8
10 wt % SiO_2	6.4	5.0	1.2	65	8.5	7.6
20 wt % SiO_2	6.1	5.2	1.2	81	11	7.2
30 wt % SiO_2	6.5	5.5	1.1	88	12	7.5

$$\alpha(\mathrm{A/B}) = \frac{P(\mathrm{A})}{P(\mathrm{B})} = \frac{D(\mathrm{A})}{D(\mathrm{B})} \times \frac{S(\mathrm{A})}{S(\mathrm{B})} = \alpha^D(\mathrm{A/B}) \times \alpha^S(\mathrm{A/B}) \quad (5)$$

where α^D(A/B) is the diffusivity selectivity and α^S(A/B) is the solubility selectivity. The O_2/N_2 and CO_2/CH_4 permselectivities of the HBPI–silica hybrid membranes are listed in Table III, and $\alpha(O_2/N_2)$ and $\alpha(CO_2/CH_4)$ are plotted against the O_2 and CO_2 *P* values, respectively, in Figures 8 and 9.

In general, there is a trade-off relationship between the permeability and permselectivity in both glassy and rubbery polymers: the gas selectivity decreases with increasing permeability and vice versa. In Figure 9, we can see that the O_2/N_2 permselectivity of the HBPI and the HBPI–silica hybrid membranes slightly decreased when the O_2 permeability was increased, along with the upper bound trade-off line for O_2/N_2 separation demonstrated by Robeson.[41,42] That is, the free-volume holes formed by terminal modification and/or hybridization with silica were not sufficiently effective to separate O_2 and N_2, which have similar kinetic diameters and shapes. However, the HBPI–silica hybrid membranes showed relatively high $\alpha(O_2/N_2)$ values.

In contrast, the CO_2 permeability and CO_2/CH_4 permselectivity of the HBPI–silica hybrid membranes increased with increasing silica content, with a significant rise in the permselectivity for the HBPI–silica hybrid membranes with a higher degree of modification (Figure 10). These results suggest that (1) the permeability was increased by the additional formation of free-volume holes because of the crosslinking mediated by terminal modification and/or the incorporation of silica

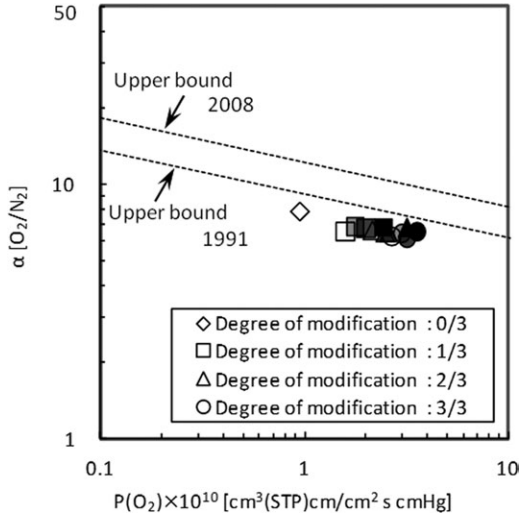

Figure 9. Ideal O_2/N_2 permselectivity [$\alpha(O_2/N_2)$] of the HPBI–silica hybrid membranes plotted against O_2 *P*.

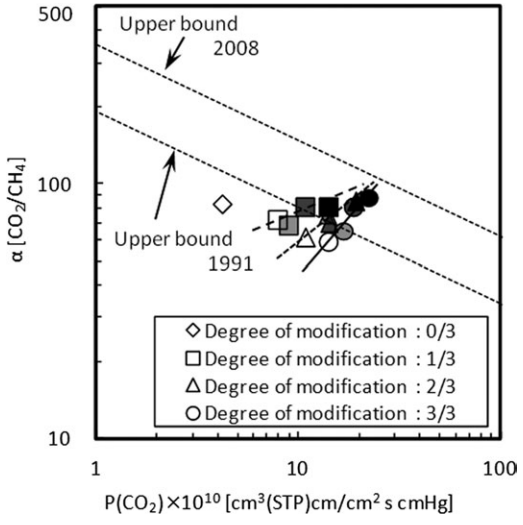

Figure 10. Ideal CO_2/CH_4 permselectivity [$\alpha(CO_2/CH_4)$] of the HPBI–silica hybrid membranes plotted against CO_2 *P*.

domains and the formation of an interfacial region by the hybridization with silica and (2) the permselectivity was increased by the characteristic distribution and interconnectivity of free-volume holes effective for CO_2/CH_4 separation. An even greater effectiveness of the incorporation of silica domains could be obtained by the homogeneous dispersion of silica nanoparticles arising from the characteristic hyperbranched structure. In addition, we concluded that the pore size of the porous silica domains formed by the sol–gel reaction in the HBPI–silica hybrids was suitable for CO_2/CH_4 separation.

CONCLUSIONS

6FDA–TAPOB HBPI–silica hybrid membranes with different degrees of modification were prepared by a sol–gel reaction, and their physical and gas transport properties were investigated. The η_{inh} values of HBPAA increased with increasing degree of modification; this suggested the formation of crosslinking through a coupling agent. The ATR–FTIR spectra revealed satisfactory imidization and sufficient formation of a three-dimensional Si—O—Si network in all of the prepared membranes. The TG–DTA measurements showed that the T_d^5s of HBPIs decreased with increasing degree of modification because of the low thermal stability of C—N bonds formed by the addition of the silane coupling agent. The DMA and TMA measurements suggested that the mobility of the HBPI molecular chains decreased in the rubbery region and that the free-volume holes of the HBPI increased in the glassy region because of the increase in the degree of crosslinking through the coupling agent. The CO_2, O_2, N_2, and CH_4 gas P values of the HBPI–silica HBD membranes increased with increasing the degree of modification and silica content; this was probably due to the additional formation of free-volume holes caused by the crosslinking mediated by terminal modification and/or the incorporation of silica domains and the formation of an interfacial region caused by the hybridization with silica. The CO_2/CH_4 permselectivity of the HBPI–silica hybrid membranes also increased with increasing silica content; this suggested a characteristic distribution and interconnectivity of the free-volume holes created by the incorporation of silica.

ACKNOWLEDGMENTS

A part of this research was supported by the Regional Innovation Strategy Support Program of the Kyoto Environmental Nanotechnology Cluster.

REFERENCES

1. Membrane Gas Separation; Yampolskii, Y., Freeman, B., Eds.; Wiley: West Sussex, United Kingdom, **2010**.
2. Kim, T. H.; Koros, W. J.; Husk, G. R.; O'Brien, K. C. *J. Membr. Sci.* **1988**, *37*, 45.
3. Stern, S. A.; Mi, Y.; Yamamoto, H. *J. Polym. Sci. Part B: Polym. Phys.* **1989**, *27*, 1887.
4. Okamoto, K.; Tanaka, K.; Kita, H.; Ishida, M.; Kakimoto, M.; Imai, Y. *Polym. J.* **1992**, *24*, 451.
5. Li, Y.; Wang, X.; Ding, M.; Xu, J. *J. Appl. Polym. Sci.* **1996**, *61*, 741.
6. Kim, Y. H. *J. Polym. Sci. Part A: Polym. Chem.* **1998**, *36*, 1685.
7. Gao, C.; Yan, D. *Prog. Polym. Sci.* **2004**, *29*, 183.
8. Jikei, M.; Kakimoto, M. *J. Polym. Sci. Part A: Polym. Chem.* **2004**, *42*, 1293.
9. Fang, J.; Kita, H.; Okamoto, K. *Macromolecules* **2000**, *33*, 4639.
10. Fang, J.; Kita, H.; Okamoto, K. *J. Membr. Sci.* **2001**, *182*, 245.
11. Gao, H.; Wang, D.; Jiang, W.; Guan, S.; *Jiang. J. Appl. Polym. Sci.* **2008**, *109*, 2341.
12. Peter, J.; Khalyavina, A.; Kříž, J.; Bleha, M. *Eur. Polym. J.* **2009**, *45*, 1716.
13. Suzuki, T.; Yamada, Y.; Tsujita, Y. *Polymer* **2004**, *45*, 7167.
14. Hybrid Materials; Kickelbick, G., Eds.; Wiley-VCH: Weinheim, United Kingdom, **2007**.
15. Zou, H.; Wu, S.; Shen, J. *Chem. Rev.* **2008**, *108*, 3893.
16. Cornelius, C. J.; Marand, E. *J. Membr. Sci.* **2002**, *202*, 97.
17. Ragosta, G.; Musto, P. *eXPRESS Polym. Lett.* **2009**, *3*, 7, 413.
18. Romero, A. I.; Parentis, M. L.; Habert, A. C.; Gonzo, E. E. *J. Mater. Sci.* **2011**, *46*, 4701.
19. Boroglu, M. S.; Gurkaynak, M. *A. Polym. Adv. Technol.* **2011**, *22*, 545.
20. Suzuki, T.; Yamada, Y. *J. Polym. Sci. Part B: Polym. Phys.* **2006**, *44*, 291.
21. Suzuki, T.; Yamada, Y.; Sakai, J. *High Perform. Polym.* **2006**, *18*, 655.
22. Suzuki, T.; Yamada, Y. *High Perform. Polym.* **2007**, *19*, 553.
23. Suzuki, T.; Yamada, Y. *J. Appl. Polym. Sci.* **2013**, *127*, 316.
24. Takeichi, T.; Stille, J. *K. Macromolecules* **1986**, *19*, 2093.
25. Van Krevelen, D. W., Eds.; Properties of Polymers; Elsevier: Amsterdam, **1990**; Chapter 4, p 71.
26. Prabhakar, R. S.; Freeman, B. D.; Roman, I. *Macromolecules* **2004**, *37*, 7688.
27. Muruganandam, N.; Koros, W. J.; Paul, D. R. *J. Polym. Sci. Part B: Polym. Phys.* **1987**, *25*, 1999.
28. Morisato, A.; Shen, H. C.; Sankar, S. S.; Freeman, B. D.; Pinnau, I.; Casillas, C. G. *J. Polym. Sci. Part B: Polym. Phys.* **1996**, *34*, 2209.
29. Weinkauf, D. H.; Kim, H. D.; Paul, D. *R. Macromolecules* **1992**, *25*, 788.
30. Chen, H.; Yin, J. *J. Polym. Sci. Part A: Polym. Chem.* **2002**, *40*, 3804.
31. Hibshman, C.; Cornelius, C. J.; Marand, E. *J. J. Membr. Sci.* **2003**, *211*, 25.

32. Tomokiyo, N.; Yamada, Y.; Suzuki, T.; Oku, J. *Polym. Prep. Jpn.* **2006**, *55*, 5175.
33. Ogata, M.; Kinjo, N.; Kawata, T. *J. Appl. Polym. Sci.* **1993**, *48*, 583.
34. Suzuki, T.; Yamada, Y. *Polym. Bull.* **2005**, *53*, 139.
35. Suzuki, T.; Yamada, Y.; Itahashi, K. *J. Appl. Polym. Sci.* **2008**, *109*, 813.
36. Park, H. B.; Kim, J. K.; Nam, S. Y.; Lee, Y. M. *J. Membr. Sci.* **2003**, *220*, 59.
37. Andrady, A. L.; Merkel, T. C.; Toy, L. *G. Macromolecules* **2004**, *37*, 4329.
38. Takahashi, S.; Paul, D. *R. Polymer* **2006**, *47*, 7535.
39. García, M. G.; Marchese, J.; Ochoa, N. A. *J. Appl. Polym. Sci.* **2010**, *118*, 2417.
40. Freeman, B. *D. Macromolecules* **1999**, *32*, 375.
41. Robeson, L. M. *J. Membr. Sci.* **1991**, *62*, 165.
42. Robeson, L. M. *J. Membr. Sci.* **2008**, *320*, 390.